Fuel 348 (2023) 128484

Contents lists available at ScienceDirect

Fuel

journal homepage: www.elsevier.com/locate/fuel

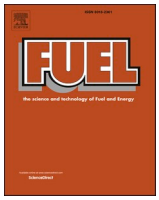

Full Length Article

Analysis of energy, exergy and CO_2 emissions in a fiberglass furnace with oxy-fuel combustion

Yuan Yao [a,b], Jun-yao He [c], Qi Chen [b], Teng Li [a,d], Bo Li [a], Xiao-lin Wei [a,d]

[a] State Key Laboratory of High Temperature Gas Dynamics, Institute of Mechanics, Chinese Academy of Sciences, Beijing 100190, China
[b] School of Mechanical, Electronic and Control Engineering, Beijing Jiaotong University, Beijing 100044, China
[c] School of Energy and Power Engineering, Xi'an Jiaotong University, Xi'an 710049, China
[d] School of Engineering Science, University of Chinese Academy of Sciences, Beijing 100049, China

ARTICLE INFO

Keywords:
Energy and exergy efficiency
CO_2 emission
Heat recovery
Oxy-fuel combustion
Fiberglass melting furnace

ABSTRACT

Energy savings and emission reductions in the building materials industry are key components of China's "dual carbon" goals. A new mathematical model of material, energy, exergy, and carbon flows was established and verified against operational data for an 80600 t/y fiberglass furnace in China. The model enables thermal budget calculation along different paths and analysis of the losses and saving potential of the entire fiberglass melting furnace and its three major subsystems. The results indicated that the selected fiberglass furnace attained a satisfactory performance with a specific energy consumption of 4.63 MJ/kg and an energy efficiency of 74.76%. Oxy-fuel combustion provided a substantial overall fuel reduction relative to air combustion. Moreover, the exergy efficiency and effective exergy efficiency reached 62.85% and 55.23%, respectively. The heat recovery system increased the exergy efficiency by 11.01%. Furthermore, the CO_2 emissions associated with glass production, major contributors, CO_2 reduction potential, and economic impact were obtained. Finally, a sensitivity analysis of the combustion chamber was conducted. This approach could identify the degree of resource and energy utilization and support the implementation of energy and exergy efficiency improvement and CO_2 emission reduction schemes.

1. Introduction

Fiberglass products are widely employed in construction, daily use, medicine, nuclear engineering, and other fields [1,2]. In 2021, the fiberglass production in China reached 6.24 million tons, with a growth rate of 15.3%. The production in China accounts for 65.68% of the global fiberglass production, and the production capacity is continuously growing. The fiberglass industry is also one of the most energy-intensive industries among those related to architectural materials. Large energy distribution differences have been observed among the final unit energy consumption values of relatively mature fiberglass factories with various capacities at home and abroad [3,4], indicating that the potential for energy efficiency enhancement still exists in China. Several scientific and engineering methods [5–9] targeting the determination, quantification and prioritization of possible energy savings in complex and large-scale industrial processes have been developed or are under continuous development. This further suggests the existence of several energy and exergy efficiency improvements and CO_2 emission reductions [10–13].

Glass melting furnaces constitute the core of energy consumption in fiberglass production lines. The glass melting process consumes more than 60% of the total energy input in the glass industry [14]. To facilitate the optimization of furnace design and operating conditions, a series of mathematical models of material and energy flows in the glass melting process have been proposed in the glass industry [15,16]. Authors [14,17–20] have considered a universal dynamic description of glass furnaces. Energy flow analyses studies of the outputs of different glass furnaces have been performed, as summarized in Table 1. Basically, 3–8 output items have been considered. Regarding the effective energy, the heat of four components (water evaporation, endothermic fusion reaction, melt recirculation at the working end and glass melt net heat enthalpy) always exceeds 40% of the total heat required and usually ranges from 42.2% to 53.49%. In terms of the energy loss, the majority of the total energy input escapes with the emitted flue gas, usually ranging from 15.43% to 70%. The wall loss is also a crucial part of the total energy loss and typically ranges from 14.4% to 40% of the total energy input. Finally, other heat losses account for less than 8.3% of the total energy input. However, material and energy balance analysis

E-mail address: xlwei@imech.ac.cn (X.-l. Wei).

https://doi.org/10.1016/j.fuel.2023.128484
Received 14 December 2022; Received in revised form 23 March 2023; Accepted 18 April 2023
Available online 28 April 2023

Table 1
Energy balance of outputs in different glass furnaces.

Number	1	2	3	4	5	6
Author	Limpt and Beerkens [14]		Díaz-Ibarra et al. [17]	Sardeshpande et al. [18]	Giuffrida et al. [19]	Yazawa et al. [20]
Country	Netherlands		Colombia	India	Italy	USA
Year	2012		2013	2007	2018	2017
Furnace type	Float	Container	Day tank	Container	Oxy-fuel	Glass melt pool
Furnace capacity	/	/	1.134 t/d	100.00 t/d	100.00 t/d	500.00 t/d
Water evaporation	1.40%	1.34%	0–25.00%	2.20%	53.49%	77.64%
Endothermic fusion reaction	8.10%	2.33%		6.80%		
Heat of melt recirculation at the working end	3.70%	/		40.80%		
Net heat enthalpy of glass melt	29.00%	45.17%		/		
Flue gas	35.20%	29.59%	70.00%	28.10%	15.43%	
Structural loss/wall loss	14.40%	17.31%	20.00–40.00%	16.50%	31.08%	21.80%
Other losses	8.30%	4.33%	/	5.60%		0.56%
Specific energy consumption (MJ/kg melt)	6.15	3.62	31.00–42.00	3.83	2.63	2.78

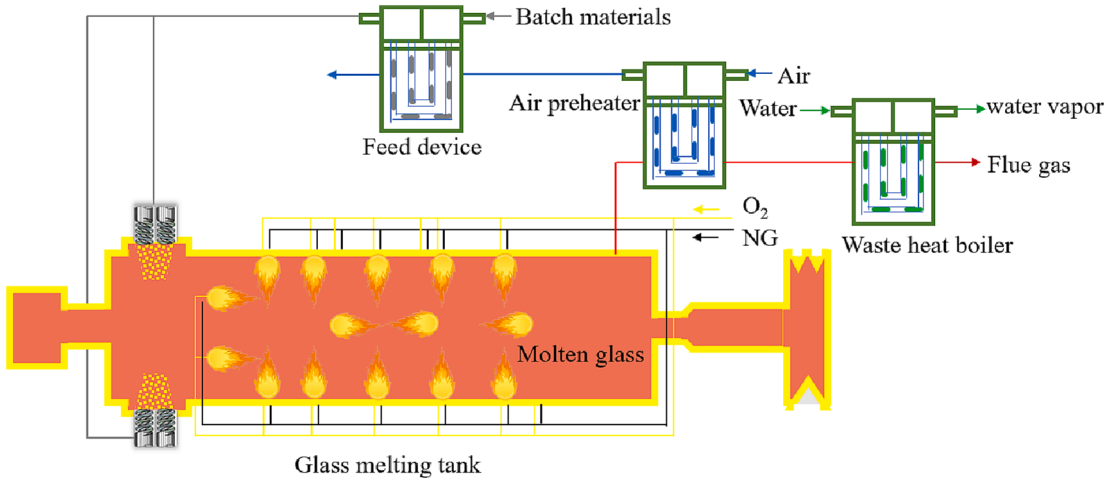

Fig. 1. Schematic of a fiberglass furnace with a heat recovery system.

processes could be further enriched and updated.

Oxy-fuel combustion has been applied to industrial furnaces to improve productivity, decrease energy consumption, and provide one of three low-cost solutions for CO_2 capture [21]. Brown [22] demonstrated that oxy-fuel combustion in certain furnaces provided a total fossil fuel reduction ranging from 50 to 70%, such as high-temperature regenerative and direct-fired furnaces. Shampand and Davis [23] proposed that the use of oxygen in glass melting could result in less CO_2. Giuffrida et al. [19] thoroughly compared the air and oxygen combustion stream mass flow rates and temperatures of glass melting furnaces and found overall natural gas savings of 23.8%. However, few material and thermal balance analysis studies have comprehensively described the components of energy savings and emission reductions in the entire glass production process.

Different furnace capacities are associated with various geometric structures and surface areas resulting in unequal smelting and refining levels at the same thermal power. Guo [24] divided 124 statistical samples of oxy-fuel glass melting furnaces in China in 2018 into four levels by capacity, and small and medium furnaces accounted for 73% of the total number of furnaces. Sardeshpande et al. [18] presented the effect of a furnace load accounting for 10% to 105% of the design load on the specific energy consumption (SEC, MK/kg), demonstrating that the higher the load is, the lower the SEC. To realistically describe a large range of furnace capacities and sizes in China, a reference for future design directions of the fiberglass industry could be provided by determining the impact of the furnace capacity on SEC.

Another thermodynamic analysis method, i.e., exergy analysis [25–27], has been employed to illustrate energy use, and this method can elucidate the scope of the exergy efficiency enhancement and the magnitude of energetic “improvement potential” [28,29]. In the study of the exergy balance in a glass furnace conducted by Lucia et al. [30], exergy losses were classified into three categories: chemical reactions, heat dissipation into the environment and heat transfer. Kozlov et al. [31] experimentally determined and compared the exergetic balance among various furnaces. The results revealed that the exergy of the fuel-combustion products, with a value of 41.6%, was the highest among those of output materials, and fuel combustion provided 21.2% irreversibility, as well as 5.8% in heat exchange. Yazawa et al. [20] and El-Behery et al. [11] conducted exergy analysis studies of the prime components in the glass melt tank and regenerator, respectively, of a glass furnace. They proposed that recovering waste energy and cleaning the regenerator could increase the efficiency. Exergy analysis studies are important to improve the effectiveness of the production process and utilize various energy-saving technologies in the fiberglass sector. However, although physical exergy has been considered, chemical exergy has rarely assessed and distinctly influences the exergy distribution and efficiency.

Recently, there has been increasing interest in reducing the emission of pollutants [32–34], such as CO_2, in glass industrial ecology assessments to achieve mostly environmental and financial benefits. Furszyfer Del Rio et al. [35] reviewed 701 studies and then stated the interventions, benefits, and barriers for glass systems. However, there exists no consensus on the most promising technologies. Schmitz et al. [36] divided CO_2 emissions into component paths, and the emissions resulting from combustion and the carbonate decomposition process reached 0.61 Mt/y and 0.08 Mt/y, respectively, in the continuous filament glass fibers production process. Ruth and Dell’Anno [37] developed a dynamic model of CO_2 emission profiles for the 1988–2028

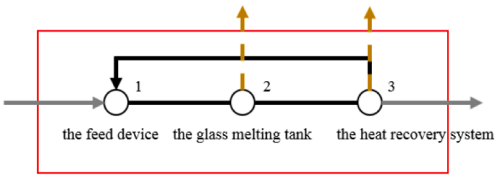

Node 1: feed device; node 2: glass melting tank; node 3: heat recovery system

Fig. 2. Network diagram of the fiberglass furnace. Node 1: feed device; node 2: glass melting tank; node 3: heat recovery system.

period and predicted emissions of approximately 0.6–1.2 t per ton glass product in 2028, including emissions resulting from electricity generation, resource extraction, manufacturing, and transportation.

In most material and energy analysis studies, the entire production process is treated as a control volume or only the melting furnace is considered, thereby ignoring the performance of the primary components inside the system, to determine the energy consumption and saving potential of internal devices in industrial furnaces. Fiberglass production steps related to energy consumption include feeding, smelting, and heat recovery processes. System analysis including the consideration of internal subsystems as calculation "nodes" provides a tool to systematically study the fundamental energy saving principle of complex energy systems and thermal processes. Yin [38] published a book titled "Theory and Methods of Metallurgical Process Integration", which is the source of this method for use in industrial production and supports its extensive application.

From the above, although considerable efforts have been devoted to investigating energy and exergy efficiency and CO_2 emissions in the container, flat glass and other industries, complete mathematical models and field data targeting efficiency improvements and emission reductions in the fiberglass industry are rare. A comprehensive analytical model of material, energy, and exergy flows and CO_2 emissions of a fiberglass furnace is presented here. The flow distributions, energy savings and CO_2 emission reduction potential are quantitatively assessed. Particular attention is directed toward the energy and exergy efficiency, CO_2 emission target and effect of furnace capacity on SEC.

2. Method

2.1. Fiberglass furnace basics

Based on the production process, a material and energy flow process for oxygen-assisted furnaces (shown in Fig. 1) is established. The fiberglass furnace is the key fiberglass production equipment component. Through heat derived from the combustion of natural gas or other fuels with air or pure oxygen, a high-temperature controllable flame can be formed in the combustion space, and the radiation of the flame produces a closed, adjustable, high-temperature environment. The furnace can be regarded as a chemical and physical reactor rank, in which raw materials such as pyrophyllite, quicklime, and quartz sand are converted through solid–liquid state reactions into new silicate compounds, and then molten glass is formed, as well as a large amount of high-temperature flue gas. An air preheater and waste heat boiler are used to recover heat from the produced flue gases, preheat the batch materials and generate steam. Materials with different chemical components are arranged in the production process to generate a material flow. Various forms of fuels provide power and heat for material flow and conversion in the melting process, corresponding to energy flow.

2.2. Network analysis

The material and energy balances of the fiberglass furnace constitute the foundation of the energy performance model. Usually, to apply the law of conservation of material and energy, appropriate control volumes should be defined. Thermodynamically, the glass melting tank, feed device and heat recovery system are treated as the system. The other tanks are excluded from the system due to their low relevance. All the material and energy interactions across the boundary of this control volume are depicted in Fig. 2, which shows a network diagram describing the fiberglass production process, in which the material, energy and exergy flows can be mathematically expressed. In Fig. 2, the three major subsystems of the fiberglass furnace are simplified into three nodes. Each node involves various parameters, which are the node characteristics. The surrounding block diagram is the control volume and separates the research system from the outside environment. The material and energy flows into and out of the furnace are denoted by solid lines. The energy flow of the thermal energy loss of different parts of the furnace is denoted by dotted lines.

2.3. Mathematical model and methodology

A complete and comprehensive mathematical model of the fiberglass furnace was established to identify and evaluate the entire fiberglass furnace system and its three subsystems. The following assumptions were made: first, the system is a steady flow process. Second, the environmental temperature and pressure are 20 °C and 1 atm, respectively. Third, the temperatures of the molten glass and flue gas are stable, respectively.

2.3.1. Material flow

The input and output materials in the control volume mainly comprise three and two parts, respectively. The input and output compositions and flow fluxes of cooling water and air in the heat exchanger remain unchanged. Based on mass conservation theory, the sum of the input material flows should equal the output at a given node. When the materials entering and leaving the node reach equilibrium, the nodal flow satisfies the following equation:

$$\Sigma_{i-1}^{M}\Sigma_{j=1}^{N}\left(m_i - m_j\right) = 0 \tag{1}$$

where M is the number of substances entering the node from another node or from outside the control volume; N is the number of substances leaving the node and entering another node or exiting the control volume; m_i is the mass flow flux of the i-th substance entering the node, kg; and m_j is the mass flow flux of the j-th substance leaving the node, kg. Since the substances that enter the node exhibit chemical (such as combustion) and physical reactions (such as phase transitions), the quantitative relationship between the components must be considered.

2.3.2. Energy flow

Based on the law of energy conservation, the sum of the input energy should equal the sum of the output energy at a given node. The energy flow in the heat recovery system can be simplified into an energy transfer device in which the energy remains constant. The input and output energies in the control volume mainly include five and eight parts, respectively. When a substance flows in and out of a node, the sensible heat of the substance accompanies it in ($Q_{\text{sen, in}}$, kJ) and out ($Q_{\text{sen, out}}$, kJ) of the node. Moreover, chemical or physical latent heat changes (Q_{lat}, kJ) occur due to chemical reactions or physical changes. Therefore, when the energy entering and leaving the node reaches equilibrium, its flow satisfies the following equation:

$$\Sigma_{i=1}^{M}\Sigma_{j=1}^{N}\left[\left(Q_{\text{sen, in}} - Q_{\text{sen, out}}\right) + Q_{\text{lat}}\right] = 0 \tag{2}$$

The energy efficiency can be defined as the ratio of the effective energy (Q_{eff}, kJ) to the total energy input (Q_{in}, kJ):

$$\eta = Q_{\text{eff}}/Q_{\text{in}} = Q_{\text{eff}}/\left(Q_{\text{sen, in}} + Q_{\text{lat}}\right) \tag{3}$$

The SEC (MJ/kg melt) can be characterized in terms of the energy consumption per unit mass of molten glass, which includes the specific

Table 2
Fiberglass furnace operating variables.

Number	Name of variable	Value
1	Furnace capacity	80600 t/y fiberglass
2	Main fuel	Natural gas
3	Combustion-supporting gas	95% oxygen
4	Flow rate of the combustion-supporting gas	3000 Nm^3/h
5	Excess air coefficient	1.15
6	Moisture content of the glass raw materials	5%
7	Input temperature of fuel, combustion-supporting gas, and batch materials	20 °C
8	Average temperature of molten glass	1420 °C
9	Temperature of the flue gas discharged from the glass melting tank	1300 °C
10	Discharged temperature of flue gas	160 °C

heat of the chemical and sensible heat of inputs and the specific power of the electric boosting device [39], and can be obtained as follows:

$$SEC = Q_{in}/m_{mg} \tag{4}$$

where m_{mg} is the mass flow flux of molten glass, kg. The upper bounds of the fuel reduction (Fuel, kg) and fuel reduction ratio (Fuel%), determined by the waste heat utilization, depend on the type of fuel used and the waste energy potential as follows:

$$\text{Fuel\%} = \text{Fuel} \times 100\% = Q_w/Q_{low} \times 100\% = (Q_1 + Q_2)/Q_{low} \times 100\% \tag{5}$$

where Q_w is the total waste heat, kJ; Q_{low} is the lower calorific value of the fuel, kJ/kg or kJ/m^3; Q_1 is the sensible heat of the batch materials, kJ; and Q_2 is the latent heat of steam in the waste heat boiler, kJ.

2.3.3. Exergy flow

The second law of thermodynamics was adopted to investigate and quantify the energy efficiency, potential, and exergy efficiency, as well as to determine the distribution of exergy destruction. Considering the environmental macroscopic flow rate $c_{f,0} = 0$ and reference height $z_0 = 0$, mechanical exergy components, such as the potential and kinetic exergy, are ignored. The stream exergy (E_x, kJ) is the sum of the physical exergy ($E_{x,\ ph}$, kJ) and chemical exergy ($E_{x,\ ch}$, kJ) [21]. It was assumed that each system stat is maintained at a constant temperature. The exergy can be calculated as:

$$E_x = E_{x,\ ph} + E_{x,\ ch} \tag{6}$$

This equation assumes a stable flowing working medium in an open system. $E_{x,\ ph}$ includes the thermodynamic energy exergy, heat exergy, and enthalpy exergy and can be expressed as:

$$E_{x,\ ph} = m[(h - h_0) - T_0(s - s_0)] = (1 - T_0/T)Q \tag{7}$$

where T_0 and T are the environmental temperature and the temperature under a given condition, respectively, K; h_j and h_0 are the enthalpies of the system under the experimental and environmental conditions, respectively, kJ/kg; s_j and s_0 are the entropies of the system under the experimental and environmental conditions, respectively, kJ/(kg·K); and Q is the available heat flux applied to the system, kJ. The chemical exergy includes the standard reaction exergy ($E_{x,\ chR}^{0}$, kJ) and diffusion exergy ($E_{x,\ chD}^{0}$, kJ) and can be computed as:

$$E_{x,\ ch} = E_{x,\ chR}{}^{0} + E_{x,\ chD}{}^{0} \tag{8a}$$

$$E_{x,\ chR}{}^{0} = -\Delta G^0 = G_R{}^{0} - G_P{}^{0} = \sum n_i g_i{}^{0} - \sum n_e g_e{}^{0} \tag{8b}$$

$$E_{x,\ chD}{}^{0} = \sum (n_e E_{x,\ e}{}^{0}) - n_{O2} E_{x,\ O2}{}^{0} \tag{8c}$$

where ΔG^0 is the difference between the Gibbs functions of the reactants and products under complete reaction, kJ; G_R^0 and G_P^0 are the Gibbs functions of reactants and products, respectively, kJ; n_i and n_e are the molar numbers of reactants and products, respectively, mol; and g_i and g_e are the standard Gibbs energies of the formation of the substances in the reactants and products, respectively, kJ/mol. The standard reaction exergy of fuel, such as methane, and the diffused exergy of three main substances (C, H, and O) of the flue gas were calculated, corresponding to chemical equilibrium states for carbon dioxide (CO_2), water (H_2O), and oxygen (O_2), respectively [40].

The exergy assessment and relevant terminology can be defined as follows: the exergy entering the system ($E_{x,\ in}$, kJ) is the fuel exergy. The exergy leaving the system ($E_{x,\ out}$, kJ) includes effective exergy and external exergy destruction. The effective exergy ($E_{x,\ eff}$, kJ) includes the exergies of molten glass and steam in the waste heat boiler. External exergy destruction comprises the exergy loss ($E_{x,\ loss}$, kJ), referring to wall dissipation and the sensible heat of the flue gas, water and vent air (one of the waste gases). This exergy flow can be recovered for application. Internal exergy destruction, referred to as irreversibility (I, kJ) [41], is an irreversible process, and this exergy cannot be utilized. The exergy balance can be expressed as follows:

$$E_{x,\ in} = E_{x,\ out} + I = E_{x,\ eff} + E_{x,\ loss} + I \tag{9}$$

The exergy efficiency [42] can be defined as the following ratio:

$$\eta_{Ex} = E_{x,\ out}/E_{x,\ in} = 1 - I/E_{x,\ in} \tag{10}$$

The effective exergy efficiency (EEE) [43] can be expressed as follows:

$$\eta_{Ex,\ eff} = E_{x,\ eff}/E_{x,\ in} = 1 - (I + E_{x,\ loss})/E_{x,\ in} \tag{11}$$

In this paper, the exergy performance coefficient (η_{IP}) is proposed, referred to as the exergetic "improvement potential", which is a dimensionless parameter associated with the exergy efficiency and EEE.

$$\eta_{IP} = (\eta_{Ex} - \eta_{Ex,\ eff})/\eta_{Ex} \times 100\% \tag{12}$$

This parameter reflects the amount and direction of exergy improvement. A large value of (η_{Ex} - $\eta_{Ex,\ eff}$) indicates that exergy loss is the main contributing factor and should be prioritized in future improvement efforts, while a small value indicates that irreversibility should be considered first.

2.3.4. CO_2 emissions

The probable total CO_2 emissions result from the combustion of fuel (e.g., natural gas) and the decomposition of carbonate, which comprises dolomite and sodium carbonate. The latter produces lower CO_2 emissions. The combustion reaction can be expressed as:

$$CH_4 + 2O_2 \rightarrow CO_2 + 2H_2O \tag{13a}$$

The chemical compositions of dolomite and sodium carbonate are $CaMg(CO_3)_2$ and Na_2CO_3, respectively. Therefore, the carbonate decomposition reactions under heated conditions can be expressed as:

$$CaMg(CO_3)_2 \rightarrow CaO + MgO + 2CO_2 \tag{13b}$$

$$Na_2CO_3 \rightarrow Na_2O + CO_2 \tag{13c}$$

In regard to thermal energy production, CO_2 emissions (CO_2) can be calculated considering the annual fuel input (m_{fuel}, kg), the average combustion efficiency ($\eta_{fuel} = 1$) and relevant stoichiometric coefficients (also referred to as emission factors, EF_{fuel}, kg_{CO2}/kg), as well as the carbonate input (m_c, fractional mass flow flux of the batch materials, kg), the decomposition efficiency ($\eta_c = 1$) and corresponding stoichiometric coefficients (EF_c, kg_{CO2}/kg). The compound CO_2 emissions [44] can be obtained as:

$$CO_2 = \Sigma(m_j \times EF_j) = m_{fuel} \times \eta_{fuel} \times EF_{fuel} + m_c \times \eta_c \times EF_c \tag{14}$$

The upper bound of CO_2 emission reductions resulting from the utilization of waste heat depends on the type of primary energy used and the waste energy potential, which are determined by the improvements

Table 3
Chemical composition of batch materials.

Chemical composition	SiO_2	Al_2O_3	Fe_2O_3	CaO	MgO	R_2O	Escaping gas	Others	Total
Mass percentage (%)	51.02	13.84	0.04	21.33	3.20	0.81	9.47	0.29	100.00

Table 4
Chemical composition of the natural gas.

Chemical composition	CH_4	C_2H_6	C_3H_8	C_4H_{10}	N_2	Others	Total
Volume percentage (%)	98.06	0.22	0.12	0.13	1.45	0.02	100.00

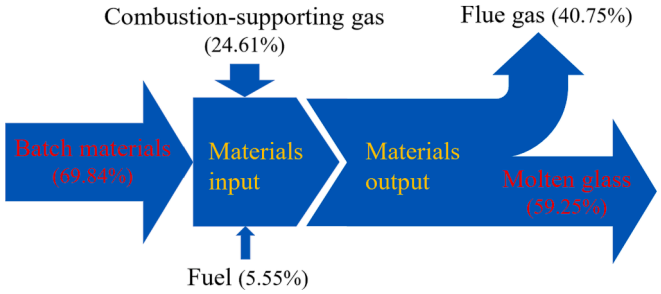

Fig. 3. Sankey diagram of the material flow split of the glass melting tank.

in energy and exergy efficiency. The avoided CO_2 emissions can be obtained as:

$$CO_2^a = \text{Fuel} \times \eta_{\text{fuel}} \times \text{EF}_{\text{fuel}} \quad (15)$$

2.4. Calculation conditions and parameters

Field studies were conducted, and data were obtained for a fiberglass production line in China. Mass and energy data were largely acquired from industry, while other data were calculated from relevant operating variables. Tables 2-4 provide the operating variables of the fiberglass furnace, the chemical composition of the batch materials and the chemical composition of the natural gas.

3. Results and discussion

3.1. Material analysis with resource utilization

The mass percentages of considering various paths into the glass smelting process under the given operating parameters were obtained. Fig. 3 shows the Sankey diagram of the material flow split of the glass melting tank. The batch materials include raw glass and chemical materials. The flue gas comprises the combustion gas products and gas escaping from the batch materials. In the oxygen-assisted fiberglass furnace, the material input includes three parts, namely, the batch materials, fuel, and combustion-supporting gas. The material output comprises two parts, namely, molten glass and flue gas. Therefore, the mass of input materials (batch materials and fuel/oxidizer) are equal to that of output materials (flue gas and molten glass) because of the process design requirements.

The total quantity is 1.68 kg/kg molten glass. Thus, the input mass is nearly 1.7 times the mass of molten glass. From a material input perspective, the quantity of the batch materials, which provide the necessary substances, is much greater than that of the fuel and combustion-supporting gas, which provide the energy determined by the process design requirements. The total mass ratio of batch materials is the highest, which is close to 70%. The conversion rate of batch materials into molten glass is 85.26%, and a small part is dissipated in the form of escaping gas due to dehydration and chemical reactions. This batch material property facilitates the production of glass with less material loss. Moreover, the mass ratio of the combustion-supporting gas is the second highest at nearly 24.61%. This result indicates that the production of 1 kg of molten glass requires a large amount of oxygen to support combustion.

Based on the material output data, the primary product (molten glass) exhibits the highest mass ratio (almost 60%). Most of the input materials are necessary. The mass ratio of the flue gas is 40.75%, and combustion gas products (the primary component of the flue gas) account for almost 30.16% of the total output. This verifies that the production of 1 kg of molten glass still generates a large amount of combustion gas products, including CO_2, water vapor, a small amount of unreacted nitrogen (from natural gas and oxygen impurities) and oxygen. Controlling combustion gas products is the key to regulating the material flow of the fiberglass furnace. Compared to the features of air combustion, oxy-fuel combustion can reduce the proportion of combustion gas products, especially the nitrogen content. The total amount of material required per kilogram molten glass is also smaller, which reduces the specific material consumption. Moreover, the mass of the gas escaping from the batch materials is a quarter that of flue gas due to the additional quantities of water vapor, CO_2 and SO_2 released through physical and chemical interactions, in which dehydration accounts for 31% of escaping gas. Finally, the mass ratio of the other system component, due to the effects of partial ablation, variations in the

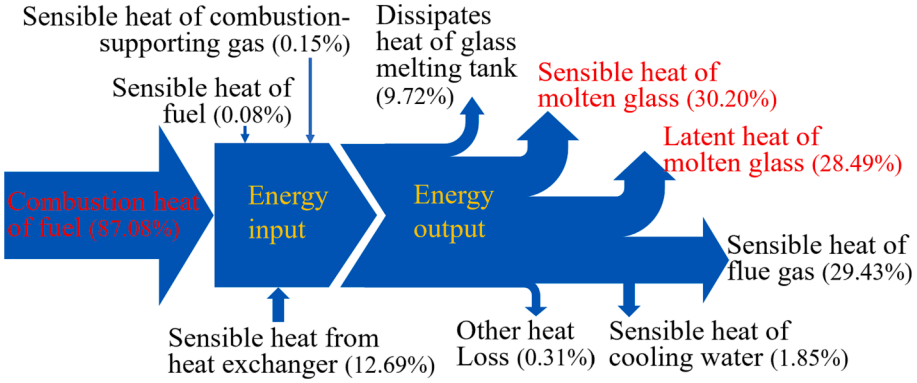

Fig. 4. Sankey diagram of the energy flow split of the glass melting tank.

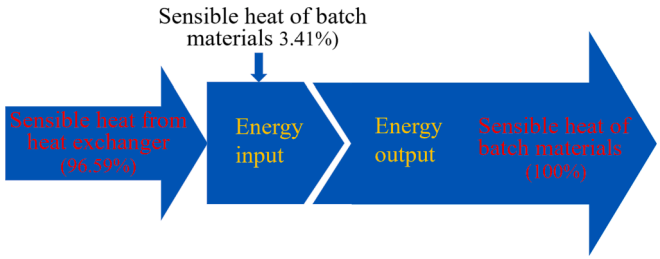

Fig. 5. Sankey diagram of the energy flow split of the feed device.

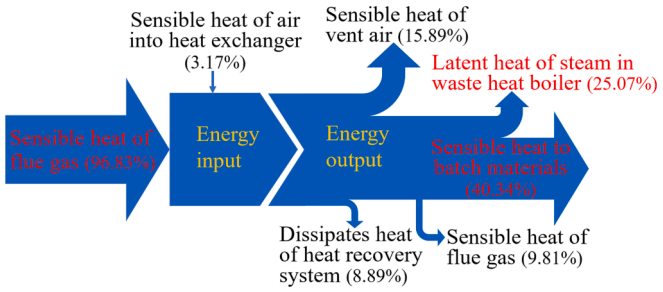

Fig. 6. Sankey diagram of the energy flow split of the heat recovery system.

composition of the raw materials and flue gas, uneven temperatures of the molten glass and flue gas, bubbling air amount, atomizing media, and leaking air, are ignored.

3.2. Energy analysis with energy utilization

3.2.1. Glass melting tank

The energy forms in the glass melting tank are almost the same as those in the entire system. However, the energy flow in the glass melting tank differs from that in the whole system because of the heat recovery system. Fig. 4 shows a Sankey diagram of the energy flow split. The total energy is 5224 kJ/kg molten glass considering waste heat recovery. Based on the energy input, most of the energy is supplied by fuel combustion (i.e., 87.08%). Another component of the energy input is the sensible heat of batch material drying and preheating by the heat exchanger, which is approximately one-seventh that of the fuel combustion. However, this part accounts for only 43.13% of the heat removed by the flue gas.

According to the energy output, the available energy in the glass melting tank offers a heat source for molten glass production and heating with a low energy efficiency of 58.69% because of the produced flue gas and dissipated heat. The heat consumption of the silicate formation reaction accounts for the highest proportion of the total heat consumption for molten glass production, indicating that this step represents an energy saving opportunity and that suitable batch materials could reduce the SEC to a certain extent by reducing the reaction heat. Moreover, high-grade waste heat escaping with the flue gas accounts for the highest proportion of the total energy loss because of the high temperature and specific heat capacity. The second highest energy loss comprises the heat dissipated from the glass melting tank due to the high tank internal temperature and large temperature difference from the environment, which identifies insulation as another energy-saving opportunity.

3.2.2. Feed device

Fig. 5 shows a Sankey diagram of the energy flow split. The total energy is 663 kJ/kg molten glass. In view of the energy input, more than 96% of the energy supplied originates from the heat recovered through the air preheater heat exchanger. Due to the energy output, the energy consumption of the batch material reheating accounts for 100% of the total energy consumption under the assumption of no heat loss.

3.2.3. Heat recovery system

The two-stage heat recovery system comprises an air preheater followed by a waste heat boiler. The air preheater absorbs the waste heat of the flue gas from 1300 ℃ to 650 ℃ for the batch material preheating. The waste heat boiler absorbs the waste heat of the flue gas from 530 ℃ to 160 ℃ for the steam generation. The stepwise reduction in the flue gas temperature fully demonstrates the heat loss reduction enhancement due to heat recovery. Fig. 6 shows a Sankey diagram of the energy flow split. The total energy is 1588 kJ/kg molten glass. From an energy input perspective, the energy supply derived from the flue gas (close to 97%) remains the dominant factor, in which the discharge rate of the combustion gas products is double that of the escaping gas.

Based on the energy output, the available energy is used to reheat the batch materials in the feed device and saturated water in the waste heat boiler. The former directly participates in glass production. The resultant energy efficiency of the heat recovery system is approximately 66%, which is slightly above that of the glass melting tank. In general, these two devices can increase the recovered energy by 13.82% and 8.59% of the total energy input and reduce the flue gas energy by 67.56%. It seems that waste heat recovery contributes to a heat supply of 9.4×10^4 GJ/y, equivalent to saving 3200 tons of standard coal. The highest energy loss (approximately 16%) is associated with the escape of the vent air into the surroundings. Air is reutilized as an indirect medium for energy recycling via the temperature difference between air import and

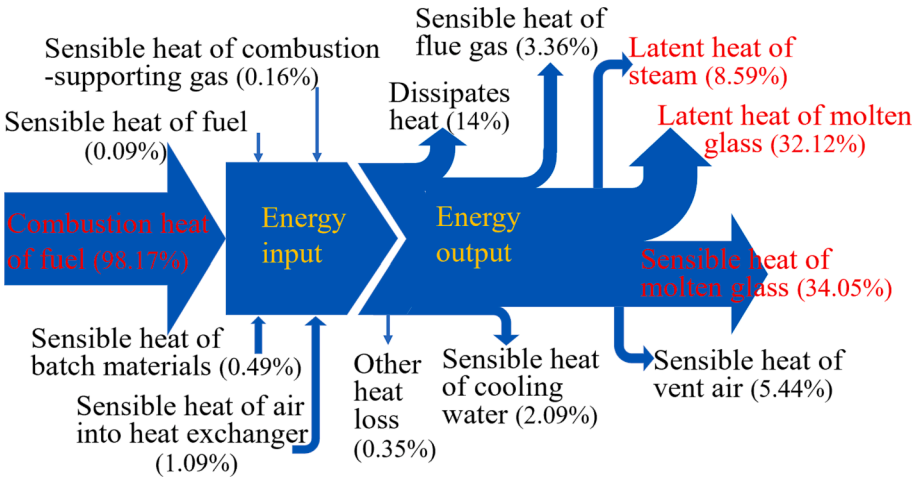

Fig. 7. Sankey diagram of the energy flow split of the fiberglass furnace.

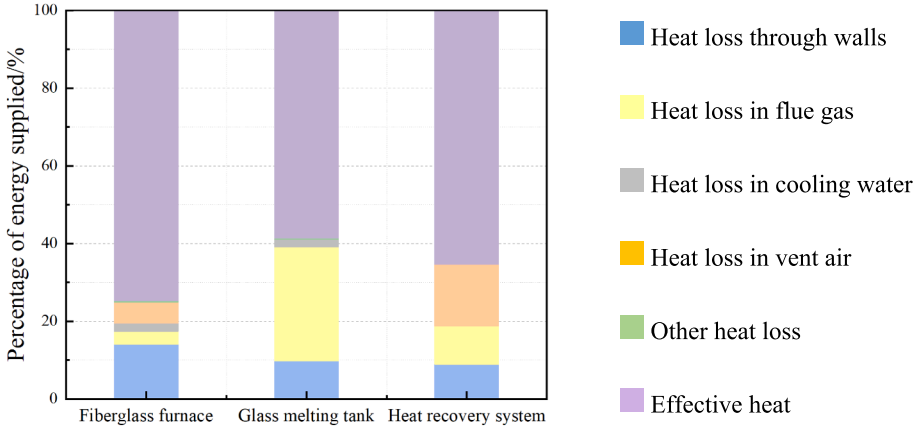

Fig. 8. Effect of the fiberglass furnace and the other two subsystems on the energy budget.

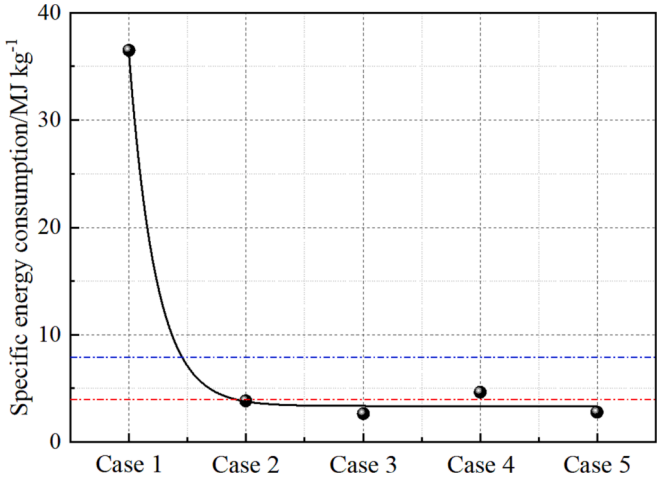

Fig. 9. SEC in the five cases.

export. Although the energy removed by the flue gas represents the second highest energy loss, this loss is less than 10% at lower temperatures, while it is lower than that of the glass melting tank, as well as heat dissipation.

3.2.4. *Whole fiberglass furnace system*

Fig. 7 shows a Sankey diagram of the energy flow split. The total energy is approximately 4634 kJ/kg molten glass. In view of the energy input, the heat energy of the fuel chemical reaction is more than 98% and is much higher than the sensible heat. The sensible heat of air into the air preheater is the second highest input, and the sensible heat of fuel is the lowest. A comparison to Fig. 3 reveals that natural gas dominates the energy ratio with a lower mass ratio. However, the amount of heat derived from the batch materials, which are the dominant raw materials and exhibit the highest mass ratio, is almost negligible, similar to the amount of heat derived from the combustion-supporting gas.

According to the energy output, almost all energy is consumed during the production of molten glass, which exhibits the highest material ratio. The useful SEC of molten glass is 3.07 MJ/kg, which accounts for more than 66% of the total energy input and exceeds the average value of 50% in the literature. Silicate formation accounts for more than 16% of the total energy output. The energy consumption of dehydration is 8.38%, which indicates the importance of drying and preheating the batch materials. Another effective consumption component is the latent heat of steam in the waste heat boiler with 2 t/h evaporation. With waste heat utilization, the total energy efficiency suggests a better performance with a value of 74.76%.

The other heat consumption component is ineffective heat, comprising the primary energy saving target. The heat dissipated by the furnace accounts for the highest proportion, which is below the average value of 20% in the literature. The furnace body heat loss accounts for the highest proportion and includes the conduction, convection and radiant heat losses across the furnace surface. Unfortunately, the nearly 100 m of flue gas pipes cause an approximately 3% heat loss. Therefore, the feeding openings, flow holes, and relevant parts are usually fully insulated to maintain a lower outer surface temperature of the furnace. The second highest energy loss is the substantial sensible heat of vent air because the batch materials are indirectly heated and due to the low energy efficiency of the heat recovery system.

The final heat losses are unavoidable, of a low grade, uneconomical, and difficult to address. The heat loss of flue gas accounts for the highest proportion, although it is far below the average value of 30% in the literature due to the low flow flux (oxy-fuel combustion) and temperature (heat recovery). This demonstrates that oxy-combustion better conforms to national principles and requirements regarding energy conservation and emission reduction than air-combustion. This process not only significantly decreases the SEC due to lowering the flue gas flux and avoiding the heat loss resulting from heating N_2 in air but also prevents N_2 from chemically reacting with O_2 in localized high-temperature zones to generate pollutants such as NO_x. Compared to the material input component, the heat loss of the combustion gas products, with the second highest mass ratio, is very low.

Fig. 8 shows the energy budget distributions of the effective and ineffective components in the fiberglass furnace and the other two subsystems. The effective heat in the fiberglass furnace increases after adding the heat recovery system and is higher in the glass melting tank than in the heat recovery system. However, the trend of the heat loss of the flue gas is the opposite. There is a significant reduction in the heat lost through the wall after heat recovery. The lower the average equipment temperature inside the system, the less heat is lost through the wall.

3.3. *Sensitivity analysis of the combustion chamber size to energy flow*

To investigate the effects of the furnace capacity (including the furnace size and production rate) on the energy efficiency, a sensitivity analysis was performed. The furnace capacity of the Chinese example considered in this paper, denoted as Case 4, is approximately 250 t/d, and the corresponding calculations were compared to the data provided in Table 1. Based on the classifications in [25], five furnaces were divided into three groups. Case 1 in Colombia with a capacity of 1 t/d pertains to a miniature furnace. Cases 2 and 3 in India and Italy, respectively, with a capacity of 100 t/d, as well as Case 4, are medium furnaces. Case 5 in the USA with a capacity of 500 t/d refers to a large

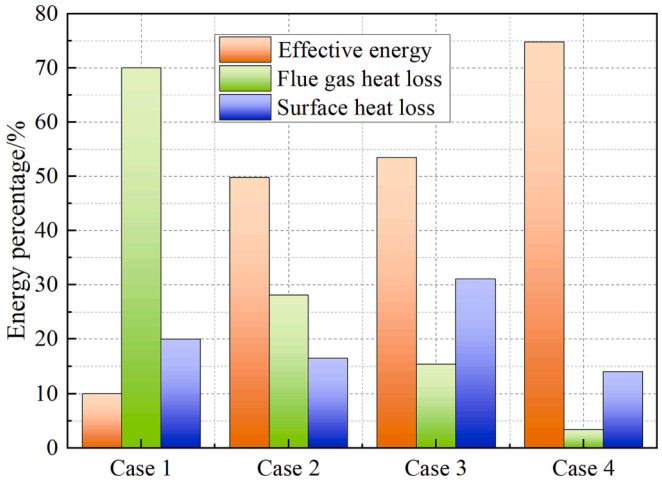

Fig. 10. Histogram of the energy percentages of three modes in the four cases.

Table 5
Furnace exergy analysis results.

			Amount (kJ/kg)	Percentage (%)
Exergy input ($E_{x,\ in}$)		Fuel exergy	4744.85	100.00
		Total	4744.85	100.00
	Effective exergy ($E_{x,\ eff}$)	Molten glass exergy	2535.27	53.43
		Exergy of steam in the waste heat boiler	85.35	1.80
		Total	2620.62	55.23
	Exergy losses ($E_{x,\ loss}$)	Surface heat dissipation	246.80	5.20
Exergy output ($E_{x,\ out}$)		Flue gas exergy	50.34	1.06
		Exergy of vent air in the heat exchanger	54.09	1.14
		Others	6.09	0.13
		Cooling water exergy	4.41	0.09
		Total	361.73	7.62
		Total	2982.35	62.85
Irreversibility (I)		Total	1762.50	37.15

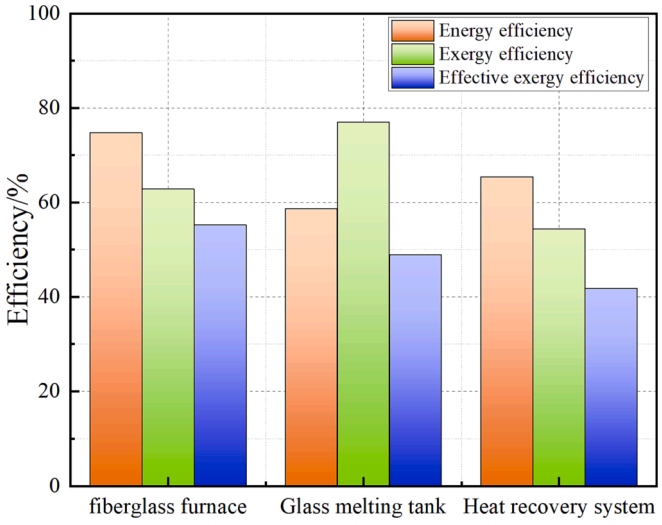

Fig. 11. Summary of the thermal analysis of the furnace and major subsystems.

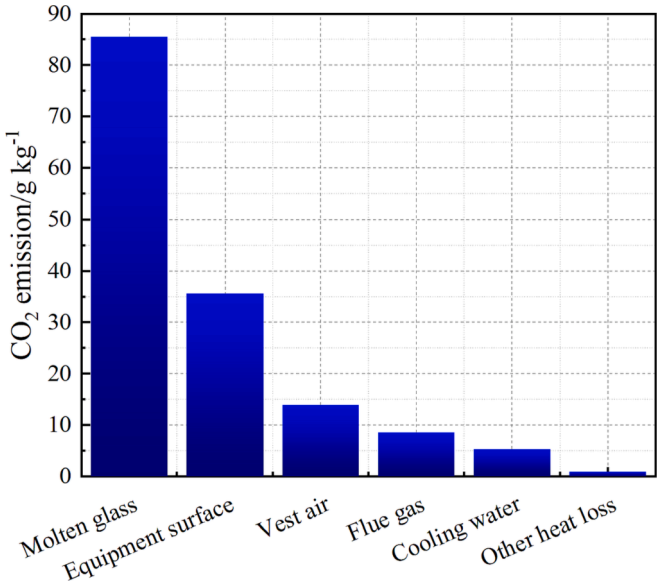

Fig. 12. CO_2 emission reduction opportunities.

furnace.

Fig. 9 shows the SECs in the five cases with different furnace capacities. Altun et al. [45] summarized the SECs of the top 10% oxy-fuel container glass furnaces in the Netherlands in 2012 in terms of performance, i.e., those with a threshold of 3.90 MJ/kg (red line). The SEC of the fiberglass furnace with heat recovery in Case 4 is approximately 4.63 MJ/kg, which is lower than the Chinese average value of approximately 7.73 MJ/kg (blue line) in 2017 [46]. However, this value does not reach the top 10% performance range and needs to be improved. The main reason is that cullets were not selected as a batch material for improvement purposes.

As shown in Fig. 9, the higher the furnace capacity is, the lower the SEC. Cases 4 and 1 differ in capacity by 250 fold, but the SEC in the former case is one-twelfth that in the latter case. This is evidence that the furnace capacity affects the energy flow, and a large furnace actually consumes less energy. The curve slightly fluctuates because the SEC is related to not only the capacity but also the furnace type, geometric structure, surface area, melting technology, and operation year [47]. It is obvious that a regular pattern applies in the glass industry and that the energy consumption can be reduced by a factor of 5%-93% while achieving considerable capital savings.

The energy percentages of the three modes of effective heat, heat removed by the flue gas and heat dissipation are compared in Fig. 10. With the variation in the furnace capacity, the energy flow of each part exhibits a general trend. The larger the furnace capacity is, the higher the proportion of the effective heat and the lower the ratio of the flue gas heat loss. This can also be attributed to oxy-fuel combustion and waste heat recovery in Case 4. The increase in energy efficiency is significant, namely, 60%. The percentage of the surface heat loss does not significantly change with the furnace capacity and fluctuates at approximately 20%.

Cases 4 and 1 differ in capacity by 250 fold, but the energy ratio of the effective heat in the former case is close to eight times that in the latter case. This is the main reason why the government requires the construction of large factories and the elimination of small furnaces. Moreover, the energy ratio of the heat removed by the flue gas in Case 4 is lower than one-twentieth that in Case 1, which reflects the high waste heat recovery potential of a small furnace.

3.4. Exergy analysis with the rate of irreversibility

The exergy can be evaluated as follows: the system performance can

Table A
Material balance of the oxygen-assisted fiberglass furnace.

Material input					Material output				
Number	Symbol	Item	Amount (kg/kg)	Percentage (%)	Number	Symbol	Item	Amount (kg/kg)	Percentage (%)
1	m_1	Batch materials	1.18	69.84	1	m_4	Molten glass	1.00	59.25
2		Glass raw materials	1.09	64.73	2	m_5	Flue gas	0.68	40.75
3		Chemical raw materials	0.09	5.11	3		Combustion gas products	0.50	30.16
4	m_2	Fuel	0.09	5.55	4		Escaping gas from batch materials	0.18	10.59
5	m_3	Combustion-supporting gas	0.41	24.61	5				
Total	m_{in}		1.68	100.00	Total	m_{out}		1.68	100.00

where m_{in} and m_{out} are the total masses per kilogram molten glass entering and leaving the node, respectively.

Table B
Energy balance of the glass melting tank.

Material input					Material output				
Number	Symbol	Item	Amount (kJ/kg)	Percentage (%)	Number	Symbol	Item	Amount (kJ/kg)	Percentage (%)
1	Q_1	Combustion heat of the fuel	4549.28	87.08	1	Q_5	Sensible heat of the molten glass	1577.61	30.20
2	Q_2	Sensible heat of the fuel	4.06	0.08	2	Q_6	Latent heat of the molten glass	1488.53	28.49
3	Q_3	Sensible heat of the combustion-supporting gas	7.61	0.15	3		Reaction heat of silicate formation	758.66	14.52
4	Q_4	Sensible heat of the batch materials	663.10	12.69	4		Heat consumption of molten glass formation	341.47	6.54
					5		Heat consumption of water evaporation from the batch materials	388.40	7.43
					6	Q_7	Sensible heat of the flue gas with 1300℃	1537.43	29.43
					7		Sensible heat of the combustion gas products	1049.68	20.09
					8		Sensible heat of the escaping gas	487.75	9.34
					9	Q_8	Dissipated heat of the glass melting tank	507.67	9.72
					10	Q_9	Sensible heat of the cooling water	96.80	1.85
					11	Q_{10}	Other heat output	16.01	0.31
Total	Q_{in}		5224.05	100.00	Total	Q_{out}		5224.05	100.00

Table C
Energy balance of the feed device.

Material input					Material output				
Number	Symbol	Item	Amount (kJ/kg)	Percentage (%)	Number	Symbol	Item	Amount (kJ/kg)	Percentage (%)
1	Q_1	Sensible heat of the batch materials	22.59	3.41	1	Q_3	Sensible heat of the batch materials	663.10	100.00
2		Sensible heat of the glass raw materials	20.94	3.16					
3		Sensible heat of the chemical raw materials	1.65	0.25					
4	Q_2	Sensible heat from the air preheater	640.52	96.59					
Total	Q_{in}		663.10	100.00	Total	Q_{out}		663.10	100.00

be optimized by minimizing the exergy losses and irreversibility. The calculated exergy analysis results for the furnace are summarized in Table 5, and the chemical exergy of the fuel is approximately 4745 kJ/kg. The exergy efficiency is 62.85%, and the EEE is 55.23%.

The exergy efficiency is 11.01% (air preheater: 9.21%; steam: 1.80%) higher than that of the furnace without heat recovery. The exergy losses are mainly due to surface heat dissipation and exergies of the flue gas, vent air, and cooling water. Surface heat dissipation exhibits the highest ratio of 5.2%. The irreversibility ratio is very high at 37.15%. Irreversibility is a restriction imposed by steps in the glass production process, such as exothermic and endothermic reactions, uncontrolled mixing phenomena, heat transfer across interfaces with finite temperature differences, and dissipation effects such as flow with friction. These irreversible phenomena should be notably considered.

Exergy analysis was conducted at both the whole system and subsystem levels to obtain the exergy distribution. Based on the exergy analysis results provided in Table 5, the improvement resulting from the various exergy losses and irreversibility is 44.77%. It is difficult to optimize the process to realize irreversibility reduction. However, exergy losses can be reduced in practice, especially surface heat dissipation. Advanced thermal insulation and sealing can reduce exergy losses.

The energy and exergy efficiencies are shown in Fig. 11. The exergy efficiency and EEE of the glass melting tank are higher than those of the heat recovery system, which suggests that the energy use quality is advanced. In the heat recovery system, the exergy efficiency and EEE are the lowest, with the irreversibility as the main source. This indicates that the energy utilization methods are unreasonable and that the heat recovery system negatively affects the exergy efficiency and EEE of the whole system. The lower exergy efficiency can be attributed to one or

Table D
Energy balance of the heat recovery system.

Material input					Material output				
Number	Symbol	Item	Amount (kJ/kg)	Percentage (%)	Number	Symbol	Item	Amount (kJ/kg)	Percentage (%)
1	Q_1	Sensible heat of the flue gas	1537.44	96.83	1	Q_3	Sensible heat from air preheater to feed device	640.52	40.34
2		Sensible heat of the combustion gas products	1049.69	66.11	2	Q_4	Latent heat of the steam in the waste heat boiler	398.11	25.07
3		Sensible heat of the escaping gas	487.75	30.72	3	Q_5	Sensible heat of the vent air in the air preheater	252.29	15.89
4	Q_2	Sensible heat of the air flowing into the air preheater	50.30	3.17	4	Q_6	Sensible heat of the flue gas with 160℃	155.75	9.81
					5		Sensible heat of the combustion gas products	105.58	6.65
					6		Sensible heat of the escaping gas	50.17	3.16
					7	Q_7	Dissipated heat of the heat recovery system	141.07	8.89
							Heat loss of the flue gas pipes	141.07	8.89
Total	Q_{in}		1587.74	100.00	Total	Q_{out}		1587.74	100.00

Table E
Energy balance of the oxygen-assisted fiberglass furnace.

Material input					Material output				
Number	Symbol	Item	Amount (kJ/kg)	Percentage (%)	Number	Symbol	Item	Amount (kJ/kg)	Percentage (%)
1	Q_1	Combustion heat of the fuel	4549.28	98.17	1	Q_6	Sensible heat of the molten glass	1577.61	34.05
2	Q_2	Sensible heat of the fuel	4.06	0.09	2	Q_7	Latent heat of the molten glass	1488.53	32.12
3	Q_3	Sensible heat of the combustion-supporting gas	7.61	0.16	3		Reaction heat of silicate formation	758.66	16.37
4	Q_4	Sensible heat of the batch materials	22.59	0.49	4		Heat consumption of molten glass formation	341.47	7.37
5		Sensible heat of the glass raw materials	20.94	0.45	5		Heat consumption of water evaporation from the batch materials	388.40	8.38
6		Sensible heat of the chemical raw materials	1.65	0.04	6	Q_8	Latent heat of the steam in the waste heat boiler	398.11	8.59
7	Q_5	Sensible heat of the air entering the air preheater	50.30	1.09	7	Q_9	Dissipated heat of the fiberglass furnace	648.74	14.00
					8		Heat loss from the furnace body	507.67	10.96
					9		Heat loss from the flue gas pipes	141.07	3.04
					10	Q_{10}	Sensible heat of the vent air in the air preheater	252.29	5.44
					11	Q_{11}	Sensible heat of the flue gas	155.75	3.36
					12		Sensible heat of the combustion gas products	105.58	2.28
					13		Sensible heat of the escaping gas	50.17	1.08
					14	Q_{12}	Sensible heat of the cooling water	96.80	2.09
					15	Q_{13}	Other heat losses	16.01	0.35
Total	Q_{in}		4633.84	100.00	Total	Q_{out}		4633.84	100.00

more of the following possible reasons: first, heat transfer intermediates remove a large amount of unused heat. Second, the preheater and boiler may not have been sufficiently heated during the previous heating period, resulting in a small temperature difference and hence a low heat transfer rate. Third, the relatively low exergy efficiency might be attributable to the reductions in both the heat transfer coefficient and heat transfer area due to the deposit layer [18,34]. Moreover, a significant difference between the exergy efficiency and EEE suggests a high "exergy potential". The exergetic "improvement potential" values of the furnace and major subsystems are 12.13%, 36.46%, and 23.23%, respectively. The η_{IP} of the glass melting tank is much larger than that of the other subsystems, which indicates that the effective exergy improvement in the glass melting tank is the greatest. The η_{IP} value of the furnace is the smallest and indicates that irreversibility is a major constraint. The lower η_{IP} is, the more thorough the effective exergy utilization and the lower the residual exergy use potential in the exergy output. Conversely, when η_{IP} is small, radically reducing the irreversibility may effectively improve the exergy efficiency.

Based on the energy and exergy analysis results above, it is important to propose specific energy conservation measures to reduce the total energy input and increase the effective efficiency. Resource utilization includes advanced burn, melt and heat recycling technologies. The recommended burn and melt technologies mainly include advanced oxy-fuel combustion and the use of batch materials such as cullets due to the lower useful energy required and primary energy input. Heat recycling can be divided into five parts considering different heat loss paths. The avoidable energy loss is essentially caused by heat dissipation from the system surface, flue gas, vent air and cooling water. Heat dissipation from the system surface is due to high wall temperatures and long flue gas pipes, which causes excessive energy dissipation into the environment. To improve the efficiency, advanced thermal insulation and shorter transport lines are suggested to lower the heat loss. The other three routes of the heat dissipation occur because of the high exit temperature and high flux. To increase the efficiency, it is necessary to choose an advanced heat exchanger and cascade waste heat recovery scheme (high, medium and low levels of heat), such as medium- and

low-temperature heat pump technologies for a lower heat loss and larger amounts of recovered energy, thus reducing the primary energy input.

The above measures are based on the original process. The following provides additional process optimization suggestions for newly built or renovated sites. First, the simplest method is to use a direct contact heat exchanger without air and an advanced cascade waste heat recovery scheme. It is possible to avoid the inevitable energy and exergy losses between multiple heat exchangers and vent air. It is assumed that the inlet and outlet temperatures of the flue gas used as a heat source remain unchanged. In contrast to indirect heating, the energy is absorbed by batch materials directly and completely from flue gas rather than from air, and the improvement in the heat recovery system is 201.99 kJ/kg molten glass with a 31.54% increase. The practical challenges during implementation involve the stability and reliability of system operation, the pipeline layout complexity and the effects of the flue gas cleanability on batch materials. Second, using more waste heat for glass melting rather than for other heat applications, such as steam generation, less commonly encountered, is another key target for reducing the primary energy consumption. It is assumed that the flue gas inlet and outlet temperatures are consistent. Instead of using the flue gas energy for steam generation, it is absorbed by batch materials, and the energy saving improvement in the whole system can reach 398.11 kJ/kg molten glass. The challenge is the large preheating area and high investment cost for gas–solid heat transfer. Third, the sensible heat of molten glass or fiberglass production should be recovered where possible. It is assumed that the sensible heat of molten glass is absorbed. The improvement in heat recovery is 1555.02 kJ/kg molten glass. The problems are that indirect heating is associated with heat loss, the process complexity is increased, and the subsequent processing technology increases the temperature control requirements of the molten glass heat exchanger. Finally, if production is intermittent, regenerators [48] or thermal storage devices should be considered. There are also studies and new technological applications related to the flue gas energy recovery [49], combustion and burners, and revolutionary melting and fining concepts.

3.5. Compound CO_2 emission analysis with heat utilization

The resource-use efficiency and carbon emission control need to be improved to meet global energy and CO_2 emission targets by 2030–2050. Calculations have indicated that the highest emission rate of 92.28% occurs when fuel is burned with a CO_2 amount of 250.09 g per kg glass, and the lowest emission rate of 7.72% occurs when carbonates are decomposed with an amount of 20.93 g/kg in the fiberglass production line. It has been estimated that the CO_2 emissions resulting from glass production can reach 2.4×10^4 t/y, which reveals a high carbon reduction potential.

In addition, the recycled waste heat can be converted to achieve a reduction in CO_2 emissions of 57.1 g/kg (5155 t/y), which corresponds to the production of approximately 0.21 kg of molten glass. Effective approaches for reducing the environmental impact include the improvement of major heat exchangers and combustion reactors and the use of alternative carbonate materials. Biological CO_2 mitigation approaches are also important, such as the use of *Chlorella vulgaris* and a nitrifier-enriched activated sludge (NAS) consortium for CO_2 capture [50] and enhancing the activity of ammonia- and nitrite-oxidizing bacteria in the activated sludge process for CO_2 mitigation [51].

According to the energy supplied, the amount of fuel savings was calculated with a waste energy potential of 2725 kJ/kg, which is based on the use of the waste energy of the molten glass, equipment surfaces, vent air, flue gas and cooling water. The CO_2 emission reduction opportunities are shown in Fig. 12. This system is expected to provide the potential to reduce the primary fuel (natural gas) consumption and CO_2 emissions by 59.89% and 55.27%, respectively. If the local heating system for glass melting is replaced by useful waste heat, the upper bound of the CO_2 emission reduction potential is approximately 1.4×10^4 t/y. Finally, the economic benefits were analyzed. The transaction price of the carbon emission allowance (CEA) listing agreement in the national carbon market is approximately 8 US dollars/t. Therefore, this value is equivalent to 0.1 million US dollars/y in revenue or cost savings for the company.

3.6. Future work and challenges

Substantial work must still be performed before the research results can be applied to plant operation optimization. First, theoretical studies should be expanded. The basic calculation method of the chemical exergy is clear, but there are few chemical exergy studies of complex reaction processes [40,52] because of the lack of initial data, such as the standard chemical exergy of elements [53]. Moreover, the conventional theoretical system is based on steady-state conditions. It is difficult to analyze the transient characteristics of certain periodically operated furnaces, such as steel converters [54]. Therefore, a more comprehensive theoretical system needs to be established for practical applications. In addition, numerical simulation and experimental research methods [18,34] are essential. Thermal analysis and mathematical models of the energy, exergy and CO_2 emissions of a furnace and each component with or without oxy-fuel combustion have been commonly used and could be popularized in the field.

Second, innovative combustion, melting, insulation and sealing, waste heat recovery and energy recovery technologies should be developed. Advanced batch materials and oxygen supply and distribution systems have been developed to improve the quantity and quality of products and reduce the SEC and pollutant emissions [3,55]. To improve the quantity and quality of heat and energy recovery, the performance of the insulation and sealing materials, exchanger and accumulator should be optimized [56,57], and heat recovery systems for high-temperature facilities, products, and slag should be added [58,59]. The level of computer-automated control of the entire process should be enhanced [60]. The promotion of greater cross-disciplinary cooperation and exchange is the key challenge limiting the development of the industry from rote mechanization to intelligent systems.

Finally, green operation and low carbon emissions are long-term themes. Oxygen-fuel combustion is beneficial to carbon capture. The volume percentages of the flue gas are 22.08% CO_2, 71.61% water vapor and less than 7% other substances. Water vapor can easily be removed through condensation. As a result, the CO_2 content approaches 78%. This provides development directions for industrial carbon capture. Of course, technical feasibility analysis and economic verification should be conducted next. In addition, carbon capture, utilization and storage schemes and industrial synergistic technologies should be vigorously developed [50,51,61,62], low-carbon process innovation and digital transformation should be promoted, and market trading of carbon emissions should be enhanced. The lack of industrial application of the above technologies is challenging.

In summary, complete mathematical models, field data and analysis results regarding energy and exergy efficiency and CO_2 emissions in the fiberglass industry at the system and subsystem level are provided here with the aim of improving efficiency and reducing emissions to enhance the glass research framework. Compared to the literatures [14,17–20], the model can be applied to complex processes combined with oxygen-fuel combustion and two forms of waste heat recovery rather than single furnaces. The model is used to research and compare oxy-fuel and air–fuel combustion systems with and without waste heat recovery. In the model, the input and output details are refined, especially the sensible heat of the batch materials, sensible and latent heat of molten glass, dissipated heat of the fiberglass furnace, and sensible heat of flue gas. Under the design conditions, the energy efficiency is improved to 74.76%. In addition, an analysis and discussion of the sources, quantity, reduction potential and cost associated with the CO_2 emissions of the fiberglass furnace are included, and the emission reduction target and direction are clarified. Finally, the chemical exergy is introduced into

thermodynamic analysis of the fiberglass industry. According to the results of the flow distribution, quantitative energy saving potential assessment findings and the effects of the furnace capacity on the SEC, modification and reconstruction suggestions are formulated.

4. Conclusion

Comprehensive details are provided of the new energy and exergy model of a fiberglass furnace and its subsystems combined with oxygen-fuel combustion and two forms of waste heat recovery methods. Moreover, the sensitivity of various factors is analyzed. The CO_2 emission and chemical exergy analysis data pertaining to fiberglass furnaces are supplemented and updated.

(1) The fiberglass furnace achieves a satisfactory performance with an SEC of 4.63 MJ/kg and an energy efficiency of 74.76%. Waste heat recovery is identified as the key aspect to save 3200 tons of standard coal and realize a highly efficient fiberglass production system.
(2) The CO_2 emissions resulting from glass production are 2.4×10^4 t/y. Fuel combustion yields the greatest contribution. This system can potentially reduce CO_2 emissions by 55.27% with a $0.1 million increase in revenue.
(3) The exergy efficiency and EEE are 62.85% and 55.23%, respectively. The heat recovery system facilitates an 11.01% exergy efficiency increase but is the main source of irreversibility.
(4) Five cases involving various countries are explored and compared. Advanced combustion, melting and heat recycling technologies are proposed for the optimization of operating parameters.

CRediT authorship contribution statement

Yuan Yao: Methodology, Formal analysis, Investigation, Writing – original draft, Writing – review & editing, Visualization. **Jun-yao He:** Validation, Data curation. **Qi Chen:** Writing – review & editing, Supervision. **Teng Li:** Supervision. **Bo Li:** Project administration. **Xiao-lin Wei:** Conceptualization, Resources, Writing – review & editing, Funding acquisition.

Declaration of Competing Interest

The authors declare that they have no known competing financial interests or personal relationships that could have appeared to influence the work reported in this paper.

Data availability

The data that has been used is confidential.

Acknowledgments

The National Key Research and Development Plan of China (NO. 2016YFB0601501) is gratefully acknowledged. The authors also wish to thank the reviewers for their careful, unbiased and constructive suggestions.

Appendix

References

[1] Guo Yun-li Xu, Yong-zheng Z-a, et al. Implementation of fiberglass in carbon fiber composites as an isolation layer that enhances lightning strike protection. Compos Sci Technol 2019;174:117–24.
[2] Diaz D, Church J, Young M, et al. Silica-quaternary ammonium "Fixed-Quat" nanofilm coated fiberglass mesh for water disinfection and harmful algal blooms control. J Environ Sci 2019;82:213–24.
[3] Beerkens R. Concepts for energy and emission friendly glass melting: Evolution or revolution in glass melting. In: Proceedings of 9th International Conference on Advances in Fusion and Processing of Glass; 2011.
[4] Beerken RGC, Limpt JV. Energy efficiency benchmarking of glass furnaces. Ceram Eng Sci Proc 2002:93–105.
[5] D'Agostini MD, Horan B. Optimization of energy efficiency, glass quality and NO_x emissions in oxy-fuel glass furnaces through advanced oxygen staging. In: Proceedings of the 79th conference on glass problems; 2018.
[6] Lu-yao Li, Jian-jun H, Huey-Jiuan L, et al. Simulation of glass furnace with increased production by increasing fuel supply and introducing electric boosting. Int J Appl Glas Sci 2020;11(1):170–84.
[7] Lu-yao Li, Huey-Jiuan L, Jian-jun H, et al. Three-dimensional glass furnace model of combustion space and glass tank with electric boosting. Mater Trans 2019;60(6):1034–43.
[8] Fiehl M, Leicher J, Giese A, et al. Biogas as a co-firing fuel in thermal processing industries: implementation in a glass melting furnace. Energy Procedia 2017;120:302–8.
[9] Choudhary MK, Purnode B, Lankhorst AM, et al. Radiative heat transfer in processing of glass-forming melts. Int J Appl Glas Sci 2018;9(2):218–34.
[10] Danieli P, Rech S, Lazzaretto A. Supercritical CO_2 and air Brayton-Joule versus ORC systems for heat recovery from glass furnaces: performance and economic evaluation. Energy 2019;168:295–309.
[11] El-Behery SM, Hussien AA, Kotb H, et al. Performance evaluation of industrial glass furnace regenerator. Energy 2017;119:1119–30.
[12] You-wang H, Hai-yong W, Xing-hua Z, et al. Accurate prediction of chemical exergy of technical lignins for exergy-based assessment on sustainable utilization processes. Energy 2022;243:123041.
[13] Li Liang, Duan Guang-bin, Liu Zong-ming, Numerical simulation of combustion space in oxygen-fuel fiberglass furnace. In: International Conference on Materials for Renewable Energy and Environment 2013;3:951-954.
[14] Limpt H V, Beerkens R. Energy recovery from waste heat in the glass industry and thermochemical recuperator. In: Proceedings of the 73rd conference on glass problems; 2012.
[15] Loch H, Krause D. Mathematical simulation in glass technology. Mainz: Springer-Verlag, Berlin Heidelberg; 2002.
[16] Wallenberger FT, Bingham PA. Fiberglass and glass technology. New York: Springer Science+Business Media; 2010.
[17] Díaz-Ibarra O, Abad P, Molina A. Design of a day tank glass furnace using a transient model and steady-state computation fluid dynamics. Appl Therm Eng 2013;52(2):555–65.
[18] Sardeshpande V, Gaitonde UN, Banerjee R. Model based energy benchmarking for glass furnace. Energ Conver Manage 2007;48(10):2718–38.
[19] Giuffrida A, Chiesa P, Drago F, et al. Integration of oxygen transport membranes in glass melting furnaces. Energy Procedia 2018;148:599–606.
[20] Yazawa K, Shakouri A, Hendricks TJ. Thermoelectric heat recovery from glass melt processes. Energy 2017;118:1035–43.
[21] Chu-guang Z, Zhao-hui L. Oxy-fuel combustion fundamentals, theory and practice. London: Elsevier; 2018.
[22] John BT. 100% oxygen-fuel combustion for glass furnaces. Ceram Eng Sci Proc 1991;12(3–4):594–609.
[23] Donald SE, Douglas DH. Application of 100% oxygen firing at Parkersburg, West Virginia. Ceram Eng Sci Proc 1991;12(3–4):610–31.
[24] Yong G. Talking about oxy-fuel combustion–Description of the present status of application of full oxy-fuel combustion technology in domestic glass industry based on data and statistics analysis (in Chinese). Glass Enamel 2018;46(5):43–8.
[25] Ozen DN, Koçak B. Advanced exergy and exergo-economic analyses of a novel combined power system using the cold energy of liquefied natural gas. Energy 2022;248:123531.
[26] Muhammad FT, Hao-yong C, Han G. Evaluating individual heating alternatives in integrated energy system by employing energy and exergy analysis. Energy 2022;249:123753.
[27] Topal HI, Tol HI, Kopaç M, et al. Energy, exergy and economic investigation of operating temperature impacts on district heating systems: Transition from high to low temperature networks. Energy 2022;251:123845.
[28] Hammon GP. Industrial energy analysis, thermodynamics and sustainability. Appl Energy 2007;84:675–700.
[29] Hammon GP. Towards sustainability: energy efficiency, thermodynamic analysis, and the 'two cultures'. Energy Policy 2004;32(16):1789–98.
[30] Lucia DM, Manfrida G. Breakdown of the exergy balance in a glass furnace. J Energy Res Technol 1990;112(2):124–9.
[31] Kozlov AS, Shutnikova LP, Kotselko RS, et al. Exergy balance of glass melting furnaces. Glas Ceram 1985;42(11–12):535–9.
[32] Rui-yu Y, Zheng-dong L, Fang-qin S-G. Thoughts on the implementation path to a carbon peak and carbon neutrality in China's steel industry. Engineering 2021;7:1680–3.
[33] Ferrer S, Mezquita A, Aguilella VM, et al. Beyond the energy balance: Exergy analysis of an industrial roller kiln firing porcelain tiles. Appl Therm Eng 2019;150:1002–15.
[34] Sardeshpande V, Anthony R, Gaitonde UN, et al. Performance analysis for glass furnace regenerator. Appl Energy 2011;88(12):4451–8.
[35] Furszyfer Del Rio DD, Sovacool B, Foley A, et al. Decarbonizing the glass industry: A critical and systematic review of developments, sociotechnical systems and policy options. Renew Sustain Energy Rev 2022;155:111885.

[36] Schmitz A, Kamiński J, Scalet BM, et al. Energy consumption and CO_2 emissions of the European glass industry. Energy Policy 2011;39(1):142–55.
[37] Ruth M, Dell'Anno P. An industrial ecology of the US glass industry. Resour Policy 1997;23:109–24.
[38] Rui-yu Y. Theory and methods of metallurgical process integration. Beijing: Metallurgical Industry Press; 2016.
[39] Raic J, Gaber C, Wachter P, et al. Validation of a coupled 3D CFD simulation model for an oxy-fuel cross-fired glass melting furnace with electric boosting. Appl Therm Eng 2021;195:117166.
[40] Huang YW, Mei-qian C, Li QH, Xing W. A critical evaluation on chemical exergy and its correlation with high heating value for single and multi-component typical plastic wastes. Energy 2018;156:548–54.
[41] Wei-jia H, Yu-fei L, Dan-xing Z, et al. Exergy-environment assessment for energy system: Distinguish the internal and total exergy loss, and modify the contribution of utility. Energ Conver Manage 2022;251:114975.
[42] Xiu-wen S, Yun Z, Shu-ai S, et al. Exergetic life cycle assessment of cement production process with waste heat power generation. Energ Conver Manage 2014; 88:684–92.
[43] Krishnan MG, Rajkumar S. Effects of dual fuel combustion on performance, emission and energy exergy characteristics of diesel engine fuelled with diesel-isobutanol and biodiesel-isobutanol. Energy 2022;252:124022.
[44] Fraia SD, Macaluso A, Massarotti N, et al. Energy, exergy and economic analysis of a novel geothermal energy system for wastewater and sludge treatment. Energ Conver Manage 2019;195:533–47.
[45] Conradt R. Prospects and physical limits of processes and technologies in glass melting. J Asian Ceram Soc 2019;7:1–20.
[46] Zhi-wei Li, Xiu-jin He, Yong-qing W, et al. Design of a flat glass furnace waste heat power generation system. Appl Therm Eng 2014;63:290–6.
[47] Altun GC, Basol AM. Numerical analysis of the radiant heating effectiveness of a continuous glass annealing furnace. Appl Therm Eng 2022;204:117943.
[48] Reboussin Y, Fourmigue JF, Marty Ph, et al. A numerical approach for the study of glass furnace regenerators. Appl Therm Eng 2005;25(14–15):2299–320.
[49] Reboussin Y, Fourmigue JF, Marty Ph, et al. Multigeneration system exergy analysis and thermal management of an industrial glassmaking process linked with a Cu-Cl cycle for hydrogen production. Int J Hydrogen Energy 2019;44:9791–801.
[50] Sepehri A, Sarrafzadeh MH, Avateffazeli M. Interaction between Chlorella vulgaris and nitrifying-enriched activated sludge in the treatment of wastewater with low C/N ratio. J Clean Prod 2020;247:119164.
[51] Sepehri A, Sarrafzadeh MH. Activity enhancement of ammonia-oxidizing bacteria and nitrite-oxidizing bacteria in activated sludge process: metabolite reduction and CO2 mitigation intensification process. Appl Water Sci 2019;9:131.
[52] Palacios-Bereche R, Gonzales R, Nebra SA. Exergy calculation of lithium bromide-water solution and its application in the exergetic evaluation of absorption refrigeration systems LiBr-H_2O. Int J Energy Res 2012;36:166–81.
[53] Rivero R, Garfias M. Standard chemical exergy of elements updated. Energy 2006; 31:3310–26.
[54] Sen Li, Xiao-lin Wei, Li-xin Yu. Numerical simulation of off-gas formation during top-blown oxygen converter steelmaking. Fuel 2011;90(04):1350–60.
[55] Sen Li, Yi-fei Ge, Xiao-lin W. Experiment on NO_x reduction by advanced reburning in cement precalciner. Fuel 2018;224:235–40.
[56] Bin-fan J, Zhou Fang Qu, Heng-yu X-H. Industrial waste heat recovery: A helix-weaved convection-radiation converter for heat transfer enhancement in gas heat exchanger. Chem Eng Process 2022;173:108853.
[57] Bing-lang R, Guang W, Hai-bin Z, Qing-guo X, Xuefeng S, Jing-song W. In-situ catalytic reforming of converter gas in converter flue based on thermochemical energy storage: kinetics and numerical simulation. J Storage Mater 2022;48: 103693.
[58] Haghanimanesh M, Baniasadi E, Kerdabadi J K, Yu Xiao-hui. Exergoeconomic analysis of a novel trigeneration cycle based on steel slag heat recovery and biogas production in steelmaking plants. Energy Conversion and Management 2022;263: 115688.
[59] Ramirez R, Farias O. Gas extraction hood modeling in a steel converter for energy recovery using phase change materials. Appl Therm Eng 2022;214:118683.
[60] Laha D, Ye R, Suganthan PN. Modeling of steelmaking process with effective machine learning techniques. Expert Syst Appl 2015;42:4687–96.
[61] Matsumiya T. Steelmaking technology for a sustainable society. CALPHAD: Comput Coupling Phase Diagrams Thermochem 2011;35:627–35.
[62] Ruo-yu X, Shan-shan W, Geng-yu G, Dong-hui L, Wen-qi L, Rui-qin Z. Evaluation of symbiotic technology-based energy conservation and emission reduction benefits in iron and steel industry: Case study of Henan. China J Clean Prod 2022;338: 130616.